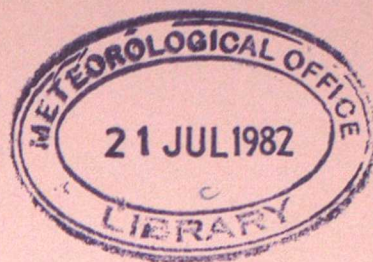LONDON, METEOROLOGICAL OFFICE.

Met.O.15 Internal Report No.46.

Results of experiments to test the performance of the Mk.II cloud condensation nucleus counter (laboratory version). By KNIGHT,K.A.

London,Met.Off.,Met.O.15 Intern.Rep.No.46, 1982,31cm.Pp.7,8 pls.4 Refs.

An unofficial document - not to be quoted in print.

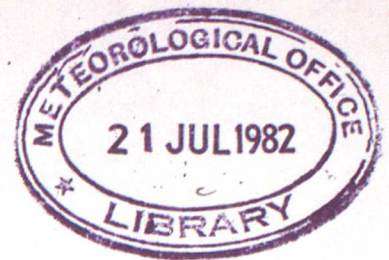# MET.O.15 INTERNAL REPORT

No. 46

RESULTS OF EXPERIMENTS TO TEST THE PERFORMANCE OF THE MKII CLOUD

CONDENSATION NUCLEUS COUNTER (LABORATORY VERSION)

by

K A Knight

JULY 1982   Cloud Physics Branch (Met.O.15)

REPORT ON EXPERIMENTS WITH THE CLOUD CONDENSATION NUCLEUS COUNTER MK II   MAY '82

1.   INTRODUCTION

The aim of these experiments was to identify any design problems with this instrument before constructing a similar model suitable for use on the C-130 aircraft. The present aircraft instrument, a modified MEE Counter, was compared with other cloud condensation nucleus (CCN) counters at the Third International Cloud Condensation Nuclei Workshop at Reno, Nevada, USA in 1980 and found to have several serious design faults. The main faults were (KITCHEN 1982):

1.   An inadequate light source giving too large a minimum detectable droplet size ($\sim 3 \mu m$) which led to an underestimate of the CCN concentration.

2.   Flow caused by turbulence and convection within the chamber.

3.   Contamination of the chamber which was practically impossible to remove.

4.   Condensation on chamber windows of light source and detector.

5.   Photodiode output susceptable to noise.

6.   Calibration procedure unsatisfactory as this cannot be done directly by photographic means.

The MK II counter (Laboratory Version) was designed to overcome these deficiencies.

2.   DESCRIPTION OF THE INSTRUMENT

The instrument is based on a thermal gradient diffusion chamber (TGDC), diameter 7cm, height 1cm. The top and bottom plates are made of black anodised alloy and covered with black absorbent paper kept wet with distilled water. (At present there is no system to keep these papers wet continually. They need to be wetted at the start of each experiment). The temperatures of these plates can be monitored via a thermistor positioned in the centre of each. The temperature in the chamber is controlled by means of a thermoelectric (Peltier) cooler device attached to the lower plate.

The chamber is illuminated by a He-Ne laser and the light scattered by the droplet cloud collected by a photodiode placed at an angle of 45° to the forward direction. The signal from this detector is then amplified and passed to a   mVoltmeter or chart recorder. The laser has the advantage of producing less unwanted heat than conventional illumination as well as having a longer lifetime.

A camera with a macro lens is placed at 90° to the illuminating beam and this is used to calibrate the instrument by manually counting the number of droplets visible in the sample volume.

A small pump draws the sample air into the chamber at low velocity via the top (warm) plate. This helps to reduce problems due to transient supersaturations. The exhaust gas exits the chamber via pipes from the chamber walls. A more powerful pump can be used to purge the lines of the previous air sample.

A typical cycle is as follows:

a.   The current to the Peltier Coolers is adjusted until the desired ΔT is obtained (the upper and lower temperatures can be displayed on a digital meter).

b.   The line pump is operated to purge the lines (if desired).

c.   With the laser activated the chart recorder is started giving a reading of the background signal from the photodiode.

d.   The sample pump is operated for about 5 seconds.

e.   The camera is operated when a peak is detected on the chart recorder or mVoltmeter (if calibration is required).

f.   The supersaturation is calculated from the temperature readings and the CCN count is obtained from either the peak voltage on the chart recorder or by counting the number of droplets visible on the film.

3.   THEORY

The light intensity (I) scattered by a droplet cloud in the chamber when illuminated by a monochromatic beam of light is often assumed to follow in relation.

$$I = CNr^2 \qquad\qquad (1)$$

where C = constant, N = number of droplets in the beam, and r = radius of the droplets (LALA + JUISTO 1977).

However, this relation is only approximate, as light scattered by a cloud of small droplets produces 'Mie' peaks, their intensity being a function of droplet size, scattering angle, refractive index of the droplets, and the wavelength of radiation. With white light, as used in the present aircraft instrument, these Mie peaks are smoothed out partly due to angular integration and also due to the range of droplet sizes and variations in wavelength. Using monochromatic light, however, it was not clear whether these Mie peaks would be evident. Obviously if Mie peaks did occur they would make calibration of the instrument difficult.

A program to calculate scattering properties of a cloud of droplets was developed by SLINGO & SCHRECKER (1980) and this was modified to calculate the phase function and intensity of the scattered radiation as a function of radius (size parameter) and scattering angle for a monodisperse cloud of droplets. The results are shown later.

The other equations used by LALA & JUISTO to describe the growth of droplets in the cloud chamber are:

$$\frac{rdr}{dt} = GS \qquad\qquad (2)$$

This is a simplified form of Mason's droplet growth equation where r = droplet radius, G = constant ($\sim 10^{-12}$), S = supersaturation, t = time.

Assume droplets fall according to stokes law,

$$\text{then } V = Br^2 \qquad\qquad (3)$$

where V = velocity, B = constant and if the number of droplets in the beam at time t is given by

$$\frac{dN}{dt} = -\frac{V\,No}{h} \qquad\qquad (4)$$

where h = height of beam and No = number of droplets initially in beam, then combining equations (1) ――― (4) we obtain,

$$I = 2CGSNot \left(1 - \frac{2BGSt^2}{h}\right)$$

showing the intensity of scattered light to be a function of the number of droplets in the beam, the supersaturation, and the droplet growth time. Differentiating the above

expression produces

$$tp = \left(\frac{h}{6GSB} \right)^{\frac{1}{2}} \qquad\qquad (5)$$

and

$$Ip = \frac{4C}{3\sqrt{6}} \frac{(Gh)^{\frac{1}{2}}S^{\frac{1}{2}}No}{(B)} \qquad\qquad (6)$$

ie

$$Ip \propto S^{\frac{1}{2}}No$$

Where tp = time of maximum intensity and Ip = magnitude of the maximum intensity.

Equating equations (1) and (6)
gives

$$r^2 = 2 \frac{(Gh)^{\frac{1}{2}}S^{\frac{1}{2}}}{(6B)}$$

and using the values h = 2mm, $G = 10^{-12}m^2S^{-1}$, $B = 1.26 \times 10^8 m^{-1}S^{-1}$

$$r_p^2 = 3.25 \; S^{\frac{1}{2}} \quad \text{and} \quad t = \frac{5.293}{r_p^2} \quad \text{(from (5))}$$

where r_p (in μm) is the radius of droplets at peak intensity (assuming a monodisperse distribution in equations (1) and (2))

A graph of the rates of droplet growth is shown in figure 1. The rate of growth based on equation (2) is shown for various supersaturations and the time taken for a droplet to grow to a given size at peak intensity is also plotted.

Integrating up equation (4) and substituting for t from equation (5) gives the ratio of the number of droplets in the beam at the time of peak intensity, to that at time t = 0.

$$N = No \left(1 - \frac{2BGSt^2}{h} \right)$$

$$= No \; (1 - 1/3) \qquad \text{Substituting for t from (5)}$$

$$\frac{N}{No} = \frac{2}{3}$$

From the simple theory above it would seem that the number of activated CCN present in the beam at the time of peak intensity is only 2/3 the number present initially, 1/3 having fallen out, thus it would seem reasonable to multiply the photographic count (when calibrating the instrument) by a factor of 1.5 to obtain a better estimate of the true count. (See AYERS 1980).

3.1 RESULTS OF MIE SCATTERING PROGRAM

In the program, the refractive index used was that for water (Real 1.331, Imag 1.6410^{-8}), since this is a good approximation for weak solutions, and a wavelength of 0.6328 m (He-Ne laser). A monodisperse droplet distribution was assumed.

1. Phase function vs droplet radius

The results are shown in figure 2 for 2 scattering angles. Large peaks and troughs occur at low values of r and as the scattering angle decreases the peaks occur at larger values of r and are of greater magnitude. Between approximately .8 μm and 1.25 μm the troughs for $\theta = 35°$ and the peaks for $45°$

3

are roughly coincident. But at lower values of r the peaks (and troughs) for both $\theta = 35^o$ and 45° occur at almost the same radius. Another feature to note is the increasingly rapid fluctuations in phase function as r increases giving a smooth response at small values of r and sharp peaks at large r.

2. Averaged Intensity vs Droplet radius

Since the detector in the chamber detects scattered light over a range of scattering angles, we need to compute an average intensity over this range. The mie-scattering program was modified to calculate this intensity as a function of droplet size using

$$\overline{I} = r^2(PF(35)+PF(40)+PF(45))/3$$

Where $\overline{I}$ = average intensity, $PF(\theta)$ = phase function at angle θ, r = radius of droplets.

The results are shown in figure 3. There is a very rapid fall off in intensity below around 3μm due to the r^2 dependance. The marked peak and trough at .4-.5μm is due to the first Mie peak, shown in figure 2, where the peaks and troughs are coincident for scattering angles of 35°-45°. However between approximately 1μm and 1.9μm (the range of sizes to be detected in the chamber, corresponding to supersaturations of .1% and 1.3% respectively at peak intensity), the intensity is approximately constant with the exception of a peak at 1.2μm. Above 1.9μm the intensity increases again.

4. EXPERIMENTAL WORK

Ambient air from the laboratory was used in all the experimental work. The peak output from the photodiode was recorded on a chart recorder and the number of droplets recorded photographically on Ilford HP5 film. The sample volume was 0.0377cm^3. Eight runs were carried out (between 17 May and 1 June '82) each with 36 readings. The absorbant paper on the plates of the chamber were wetted at the start of each run and periodically renewed.

4.1 EXPERIMENT A

Measurement of peak intensity as a function of supersaturation (and therefore radius) to determine whether the theoretically predicted sensitivity (figure 3) could be verified experimentally.

Four runs were carried out. The results for the last run (Film 7) are shown in figure 4, as peak output per droplet vs radius at peak intensity. This radius was calculated from the supersaturation using the simple theory of a TGDC already described. All the results showed that the intensity is roughly constant with radius although increasing slightly with radius at larger values of r. No evidence of a Mie Peak at 1.2μm was found. Thus it would appear that the relation

$$I = CNr^2$$

is valid for monochromatic radiation scattered in the chamber at an angle of 35-45° in the forward direction over the range of supersaturations (.1% to 1.3%) to be used. The difference between the theoretical and experimental results may be due to the assumption that the droplet distribution is monodisperse. As is indicated in experiment C, this assumption is unlikely to be valid and a broader droplet spectrum would help to 'smooth out' the Mie peaks further.

4.2 EXPERIMENT B

The aim of this experiment was to investigate the hysteresis effect when increasing and decreasing ΔT. In experiment A, ΔT was decreased from a maximum to a minimum and then increased again during the run. It was noticed that some hysteresis occured, ie that for a given supersaturation the count obtained with ΔT decreasing was greater than when ΔT was increasing, which was evident when an activation spectrum (Number of drops cm^{-3} vs Supersaturation) was plotted (figure 5 is an example). Several other runs were carried out to investigate this effect. One run when ΔT was increased first to a maximum and then decreased and one run when the chamber was recycled slowly, allowing approximately 5 minutes before a reading at a new supersaturation was taken.

It was found that with rapid recycling hysteresis occured in the same sense whether ΔT was increased or decreased initially. A larger count was obtained when ΔT was decreased then when it was increased, for a given supersaturation. With slow recycling there was only hysteresis at high supersaturations (greater than about 0.6%) and this seemed to be in the opposite sense to that when the chamber was recycled quickly (figure 5A).

This hysteresis is probably due to uneven cooling of the base plate of the cloud chamber. The cooling is effected by a thermoelectric (Peltier) device in the centre of the base-plate with cooling fins across part of the plate. This will lead to the centre of the base-plate being slightly cooler than the edges when ΔT is being increased rapidly and slightly warmer than the edges when ΔT is being decreased rapidly.

Since the values of supersaturation calculated are very sensitive to temperature (an error of $.3^{o}C$ can give an error in supersaturation of 0.1%), the value of supersaturation calculated using the bottom plate temperature, as given by the thermister in the centre of the plate, will be too large if ΔT is being increased rapidly and too small if ΔT is being decreased rapidly thus giving rise to the effect seen in figure 5.

Another result of this uneven cooling may be to cause convective circulations inside the chamber, the air rising around the edges, if these are warmer than the centre (ΔT increasing). This means that the droplets in the beam at the centre of the chamber will fall out more quickly than if the air was static and not grow to their full size. This in turn will decrease the light scattered slightly and give too low a count. For ΔT decreasing, the opposite will be true.

It is thought likely that the inaccuracies in measurement of the bottom plate temperature are the main cause of the hysteresis, the circulations in the chamber being only of minor importance, since the reduction in drop size would have to be large to significantly reduce the photographic count.

4.3 EXPERIMENT C

During one of the runs for experiment A, the shutter speed of the camera was changed from $\frac{1}{4}$ to $\frac{1}{8}$ second as the supersaturation was increased (as this helps to reduce blurring of the drop images as they fall in the beam). On examining the results, it appeared that the number of CCN sampled (N) with shutter speed $\frac{1}{8}$ was nearly half that expected on the basis of a straight line fit to a graph of N Vs peak output in mV , for those readings with shutter speed $\frac{1}{4}$. When the CCN concentration with film exposured at $\frac{1}{8}$s has multiplied by 2 and plotted with the data from the film exposed at $\frac{1}{4}$s, a good straight line fit was obtained (figure 6).

A graph of number of CCN per cm^3 versus peak output voltage must necessarily be a single valued function if the scattered light intensity is to be used as a measure of the number of CCN present in a sample. Figure 7 shows such a graph for a run when the shutter speed was $\frac{1}{4}$ second throughout.

To investigate the effect of camera exposure on the number of CCN sampled by photographic means a run was carried out using three shutter speeds ($\frac{1}{4}$, $\frac{1}{8}$, 1/15) and at two different supersaturations (0.41%, 0.26%). Six frames were taken at each shutter speed, all at aperture f4.

RESULTS

Exposure(s)	No. drops per mV	
	SS=0.41	SS=0.26
$\frac{1}{4}$	12.1+.5	17.4+.9
$\frac{1}{8}$	9.1+.5	11.9+1.0
1/15	8.8+.8	10.2+.5

The above results clearly show that increasing exposure time increases the CCN count, the effect being most noticable at the low supersaturation. This implies that with larger exposure times it is possible to detect smaller droplets and therefore that the cloud of droplets is not monodisperse.

Increasing the exposure time means that the images of the droplets become blurred on the film as they fall slowly in the beam. This is obviously more of a problem at higher supersaturation where the droplets become larger more quickly and thus fall in the beam faster. Thus increasing the camera shutter speed beyond $\frac{1}{4}$s is impracticable. Problems also arise when counting the number of droplets recorded on the film, as it is almost impossible to distinguish between unactivated haze particles and very small activated nuclei. But since there are very few of these the count obtained using a exposure time of $\frac{1}{4}$s is thought to be a good measure of the CCN concentration although it will however, be slightly less than the 'true' count.

A small amount of work was done on the effect of lens aperture on the CCN count. The results were not conclusive but indicated that this is less important than shutter speed. It seems that a reduction in lens aperture does decrease the CCN count slightly especially at a shutter speed of $\frac{1}{4}$s. At $\frac{1}{8}$, and 1/15s it appears to have little effect. The conventional positioning of the camera at 90° to the beam is only for convenient construction of the chamber. Mie scattering calculations show that the scattered light intensity at 40° is roughly 15 times that at 90°. Therefore positioning the camera at 40° to incident beam symetric with the photodiode, would help to increase the minimum detectable size of droplets recorded on the film during photographic calibration.

5. CONCLUSION

The major fault with the modified MEE CCN counter used on the C-130 aircraft is the low intensity light source. This has been overcome in the MK II CCN counter (laboratory version) by using a He-Ne laser. The problems arising from Mie scattering of a monochromatic light beam by the droplet cloud have been shown (both in theory and experimentally) to be unimportant. The laser has several advantages over a conventional light source, it has a longer lifetime, a lower power requirement and produces less unwanted heat, and it can be made much lighter in weight if a laser diode is used.

The cooling of the lower plate in the MK II CCN counter was found to have problems associated with it. These appear to have been due to the uneven cooling of the plate leading to a hysteresis effect. This problem has apparently been overcome in the modified MEE instrument on the aircraft. The new aircraft counter (based on the MK II laboratory version) will therefore need a similar cooling system ie a more powerful cooling unit giving even cooling of the lower plate and electronic control of the cooling current.

Other minor faults on the modified MEE CCN counter which were corrected in the MK II version were, that the plates of the chamber, being made out of anodised alloy, were less susceptable to contamination and direct photographic calibration was provided.

Condensation on the windows of the chamber was not found to be a problem but it would be prudent to provide small heaters on the chamber windows for the camera, photodiode and laser of the new aircraft version, these being located inside the chamber walls next to the windows. These would be used to clear condensation on the windows, between runs, if it occured.

The problem of minimum detectable size of droplets linked with camera exposure time when calibrating the instrument is common to all CCN counters of this type. It is hoped that positioning the camera at 40° to the incident beam will increase the minimum detectable size and give a more accurate count. However, since there is no standard counting technique, an absolute count cannot be achieved.

REFERENCES

AYERS (1980): Static diffusion cloud chamber. Proceedings of the Third International Cloud Condensation Nuclei Workshop NASA Publication 2212

KITCHEN (1982): An Introduction and Guide to the Met O 15 CCNC Met O 15 Internal Report No 37

LALA and JUISTO (1977): An Automatic Light Scattering CCNC J.A.M. 16 p413

SLINGO and SCHRECKER (1980): A computer Program to Calculate the Properties of Light Scattering by a Cloud of Spherical Particles. Met O 15 Internal Report No 11
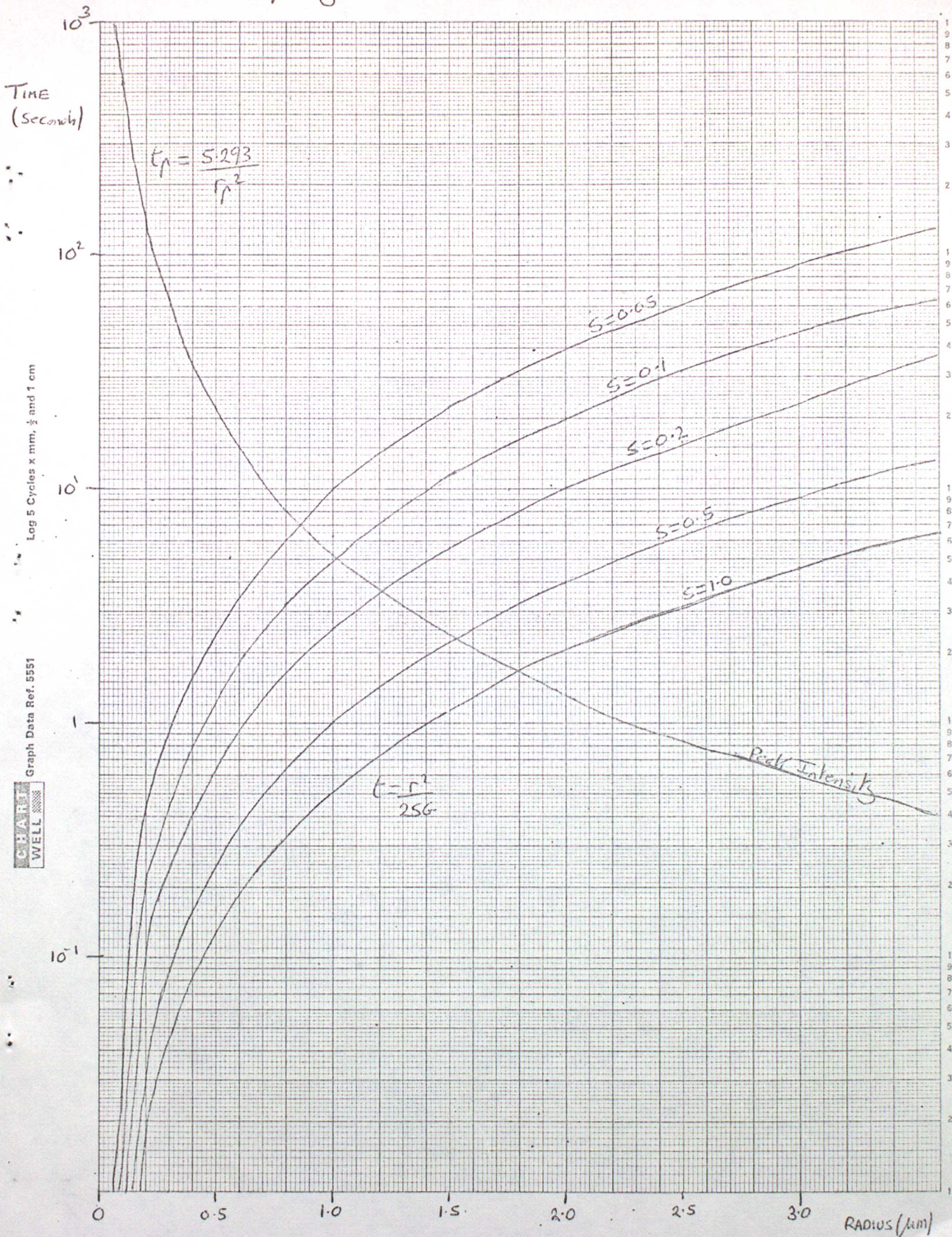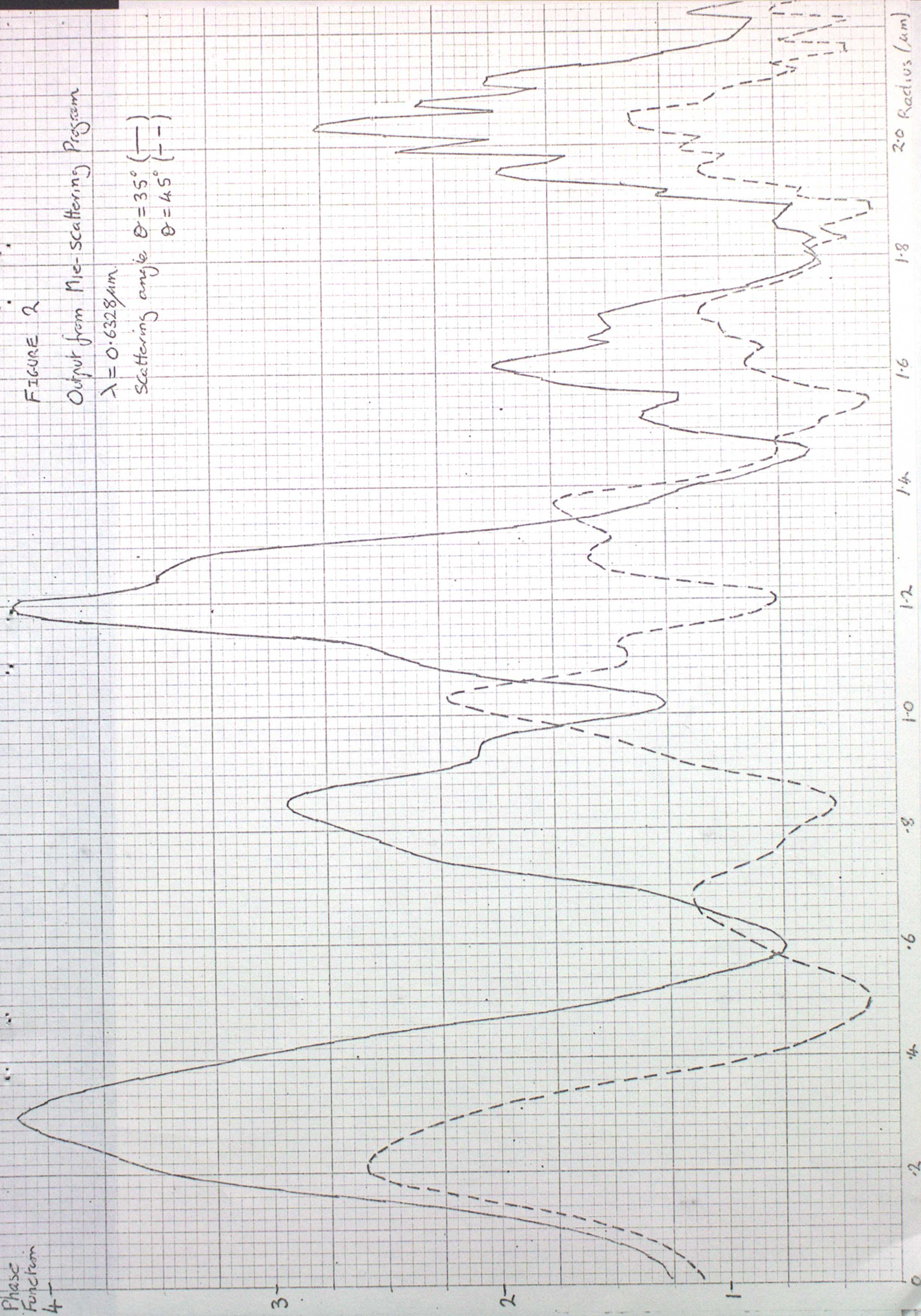
FIGURE 1

Droplet growth rates.

$$t_n = \frac{5.293}{r^2}$$

$$t = \frac{r^2}{25G}$$

S=0.05

S=0.1

S=0.2

S=0.5

S=1.0

Peak Intensity

TIME (seconds)

Log 5 Cycles x mm, ½ and 1 cm

Graph Data Ref. 5551

CHART WELL

RADIUS (μm)

FIGURE 2

Output from Mie-Scattering Program

$\lambda = 0.6328\mu m$.

Scattering angle $\theta = 35°$ (——)
$\theta = 45°$ (— —)

Phase Function

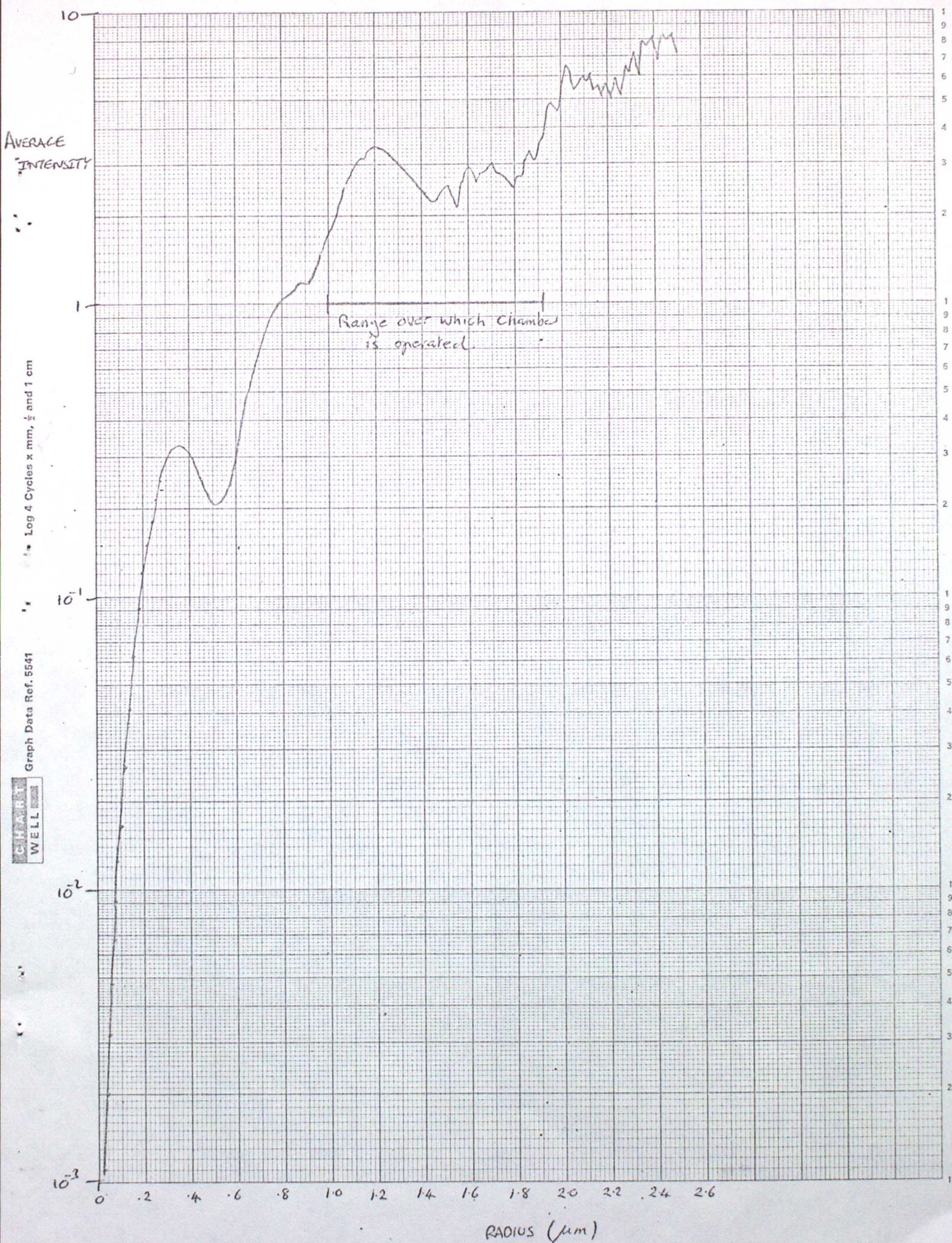2.0 Radius (μm)

FIGURE 3

Average Intensity of scattered Radiation between angles 35° and 45°

FIGURE 4: EXPERIMENT A.

Error bars represent standard error of means
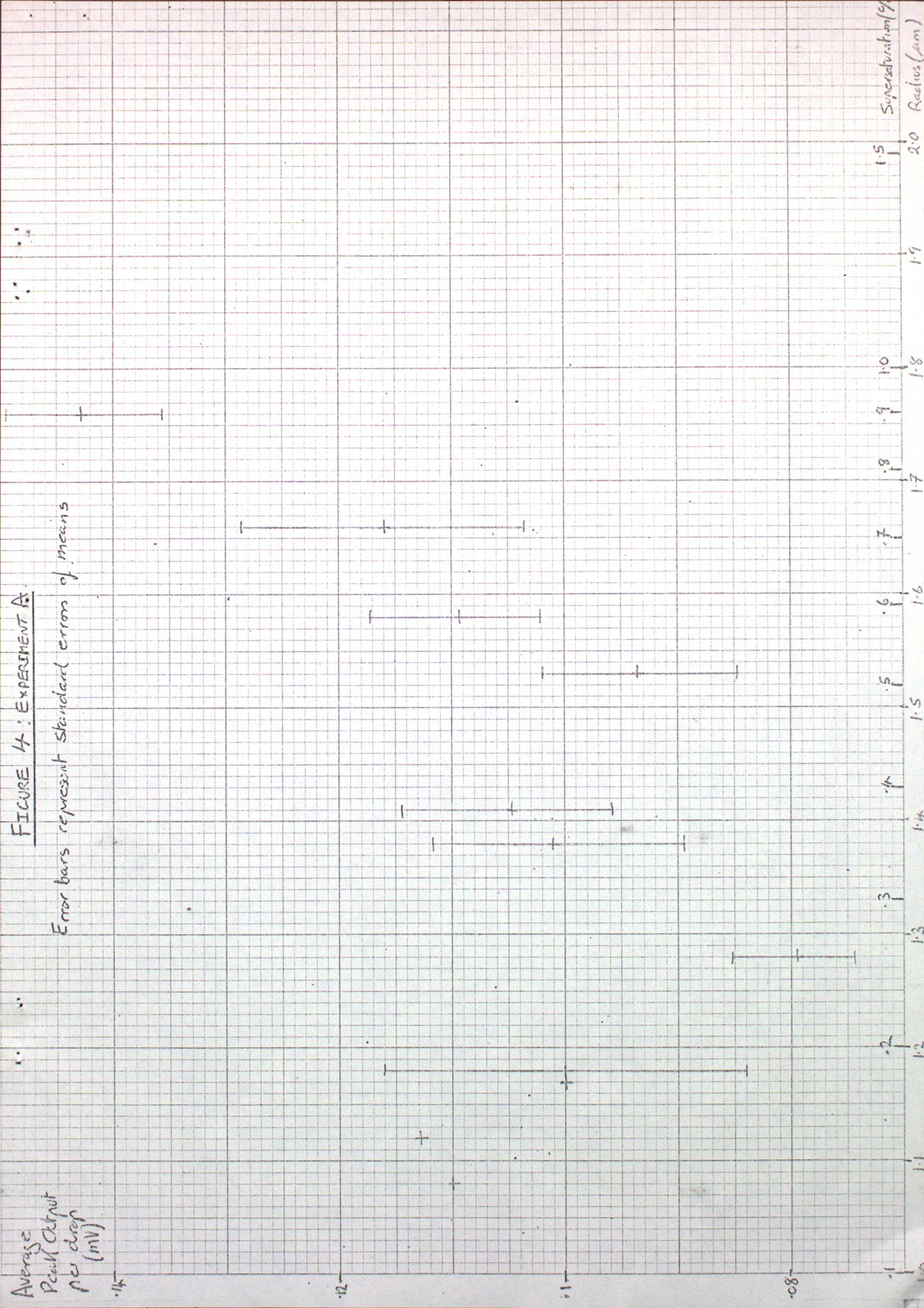
FIGURE 5

EXPERIMENT B — ACTIVATION SPECTRUM.
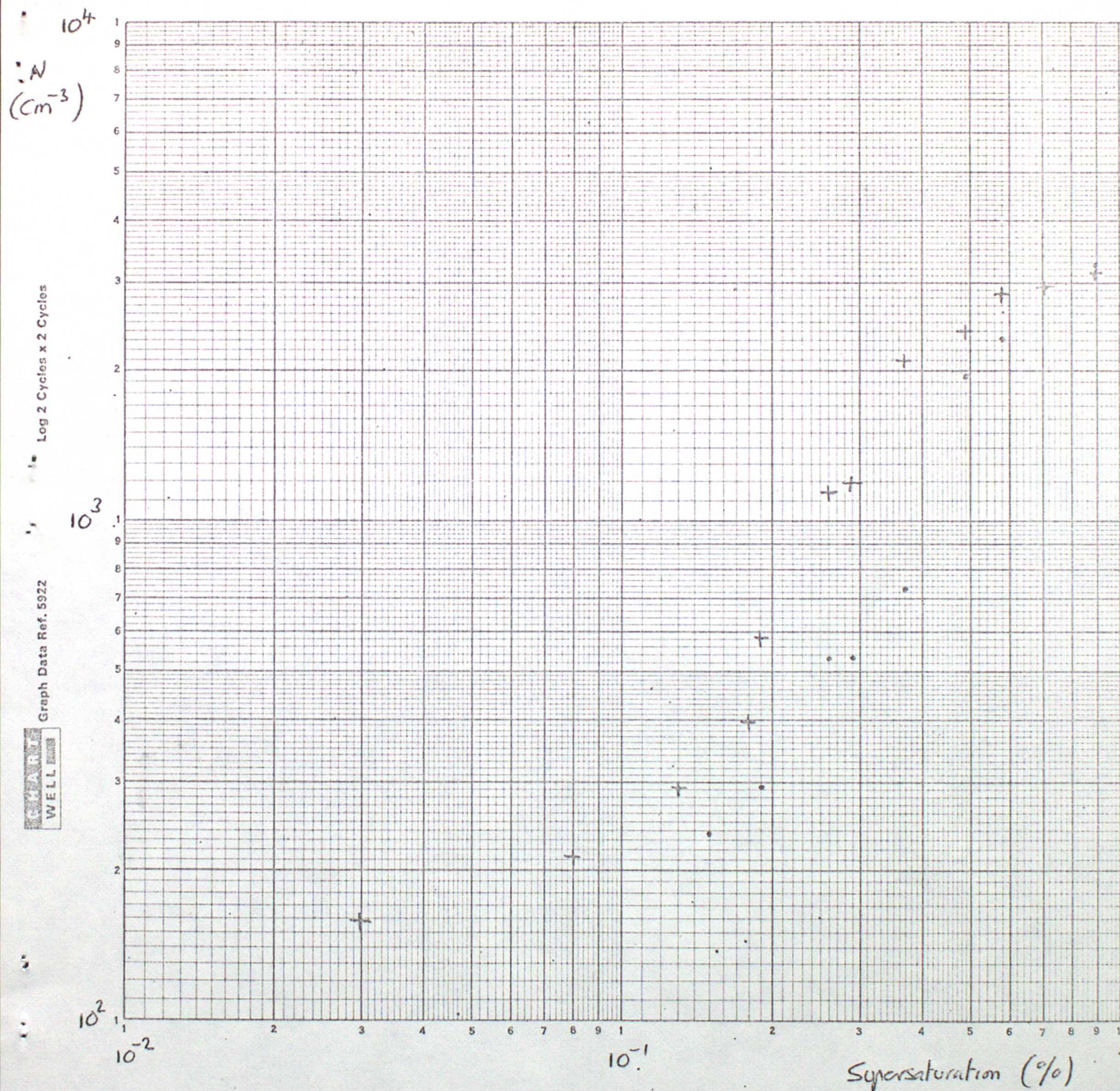RAPID RECYCLING

+ ΔT decreasing
∘ ΔT Increasing

FIGURE 5A

EXPERIMENT B — ACTIVATION SPECTRUM

SLOW RECYCLING

+ ΔT decreasing

• ΔT increasing

FIGURE 6

FIGURE 7

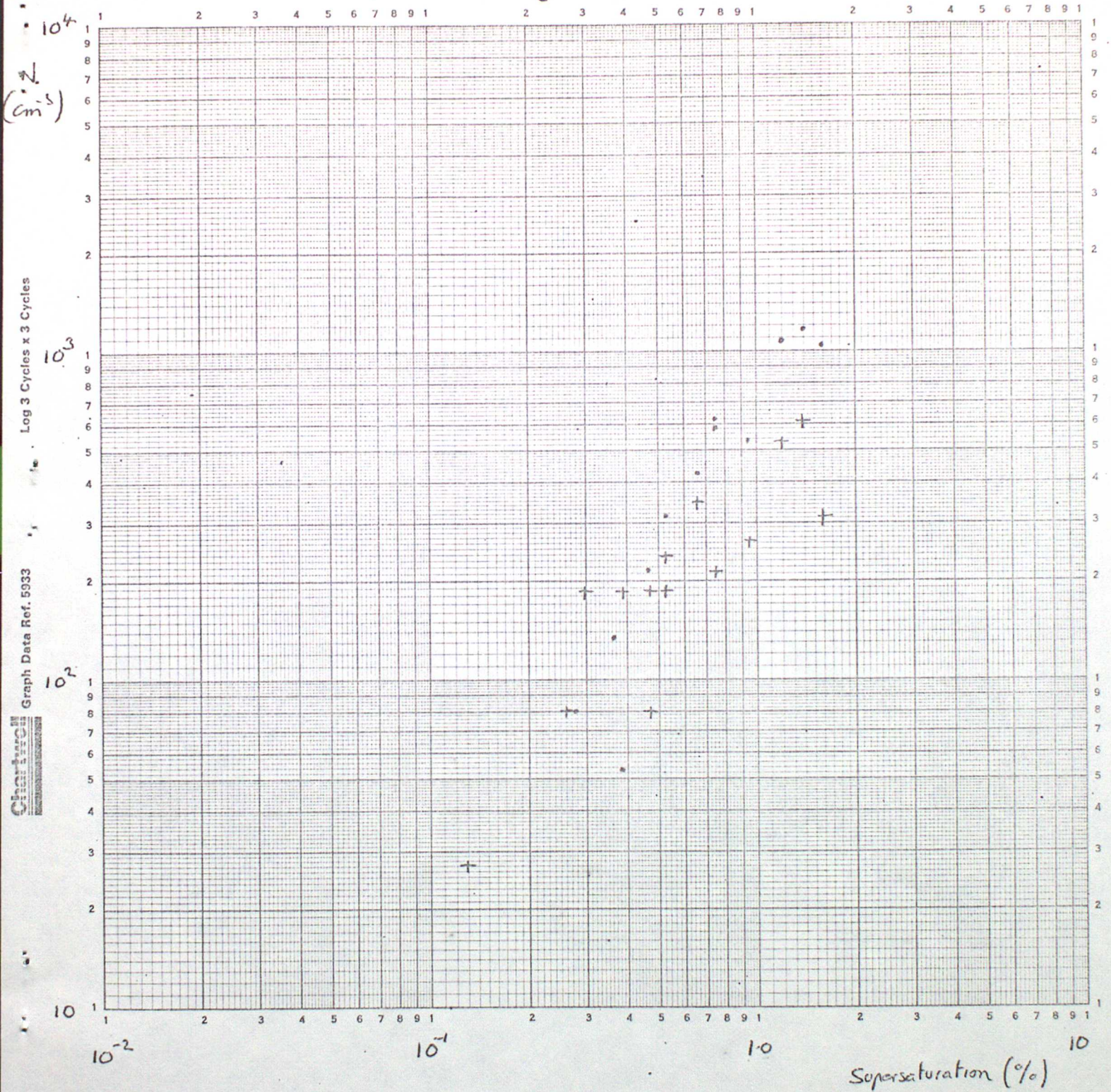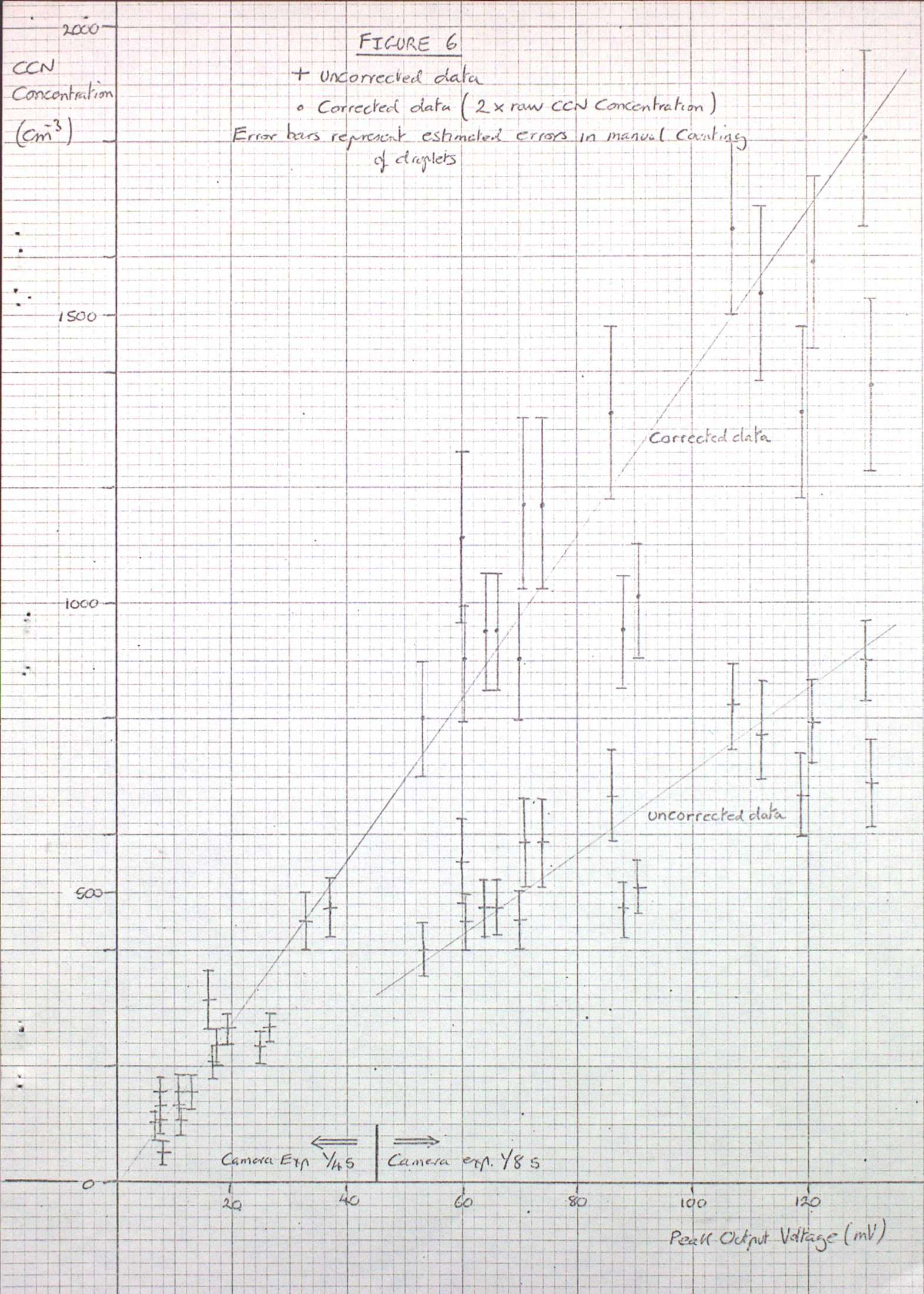Error bars represent estimated errors in manual
counting of droplets

CCN
Concentration
(Cm³)

Peak Output Voltage (mV)